Multiscale Decoding for Reliable Brain-Machine Interface Performance Over Time

Han-Lin Hsieh[1], Yan T. Wong[2], Bijan Pesaran[3] and Maryam M. Shanechi[4]

***Abstract*— Recordings from invasive implants can degrade over time, resulting in a loss of spiking activity for some electrodes. For brain-machine interfaces (BMI), such a signal degradation lowers control performance. Achieving reliable performance over time is critical for BMI clinical viability. One approach to improve BMI longevity is to simultaneously use spikes and other recording modalities such as local field potentials (LFP), which are more robust to signal degradation over time. We have developed a multiscale decoder that can simultaneously model the different statistical profiles of multi-scale spike/LFP activity (discrete spikes vs. continuous LFP). This decoder can also run at multiple time-scales (millisecond for spikes vs. tens of milliseconds for LFP). Here, we validate the multiscale decoder for estimating the movement of 7 major upper-arm joint angles in a non-human primate (NHP) during a 3D reach-to-grasp task. The multiscale decoder uses motor cortical spike/LFP recordings as its input. We show that the multiscale decoder can improve decoding accuracy by adding information from LFP to spikes, while running at the fast millisecond time-scale of the spiking activity. Moreover, this improvement is achieved using relatively few LFP channels, demonstrating the robustness of the approach. These results suggest that using multiscale decoders has the potential to improve the reliability and longevity of BMIs.**

I. Introduction

Brain-machine interfaces (BMI) decode subjects' motor intention from their neural activity. The majority of invasive BMIs use single-unit or multi-unit spiking activity as their control signal. However, the quality of the recorded spiking activity could degrade over time, for example due to scar tissue formation on the electrodes [1]. This degradation in recording quality also sacrifices BMI performance. Thus a major challenge for clinical viability is to improve the reliability of BMI performance over time. One approach to address this challenge is to exploit (in addition to spikes) other neural signal modalities in the decoder that are more robust to signal degradation over time.

In addition to spikes, another modality of neural activity that is recorded in invasive arrays is the local field potential (LFP). LFP captures cumulative network processes in the cortex and can improve longevity compared to spikes. Previous work has shown that LFP is informative of the subjects' motor intention and can be used in BMI decoding (e.g., [2]–[5]). Hence one approach to enable reliable performance is to use the recorded LFP in addition to spikes to decode intended movement.

Employing LFP and spikes simultaneously in a decoder is challenging for two main reasons [6]. First LFP and spikes have different statistical profiles. Spiking activity indicates the time-points at which action potentials are fired from neurons. Hence spike trains can be represented as a discrete-valued time-series of zeros and ones, indicating the lack or presence of spikes in consecutive time-steps, respectively. In contrast, LFP is continuous-valued and is typically processed by taking its band-powers as features. Second, the time-scales of spikes and LFP are different. While spikes happen on a millisecond time-scale, LFP usually has a slower time-scale of tens of milliseconds [2]. These difference make the simultaneous modeling of spikes and LFP challenging.

To decode spikes and LFP, one approach could be to count the number of spikes in bins in which LFP powers are computed, assume that spike counts are Gaussian-distributed, and then use a single time-scale and a Kalman filter to decode the kinematics [7]. However, recent work has shown that modeling the spikes directly using a point process filter (PPF) can improve the performance of BMIs due both to the faster control and feedback rates and to the point process encoding model [8]. These results suggest that developing multiscale decoders that take into account the different statistical characteristics and time-scales of various neural signal modalities could improve BMI performance.

Motivated by these results, we have derived such a real-time multiscale decoder [6]. Here, we show that our multiscale decoder has the potential to improve the longevity of BMI performance by utilizing spikes and LFP simultaneously. In particular, we evaluate the performance of the multiscale decoder using simultaneous motor cortical spike/LFP recorded from non-human primates (NHP) during a reach-to-grasp movement task in which all 27 degrees of freedom of the arm are monitored [9]. Prior work has shown successful decoding of joint angles in this dataset using spikes alone [9]. We consider a scenario in which some channels can no longer record spikes. We show that, compared with a PPF [10] that only uses the spikes, we can significantly improve the decoding accuracy of joint angles by exploiting the LFP activity in the multiscale decoder. Additionally, we see that performance saturates using just a few LFP channels. These results suggest that multiscale decoding could improve the longevity and reliability of BMIs.

[1,4]Han-Lin Hsieh and Maryam M. Shanechi are with the Department of Electrical Engineering, University of Southern California, Los Angeles, CA, USA (e-mail: {hanlinhs, shanechi}@usc.edu)

[2]Yan T. Wong is with the Department of Physiology, and Electrical and Computer Systems Engineering, Monash University, VIC, Australia (e-mail: yan.wong@monash.edu)

[3]Bijan Pesaran is with the Center for Neural Sciences, New York University, New York, NY, USA (e-mail: bijan@nyu.edu)

978-1-5090-2809-2/17/$31.00 ©2017 IEEE

II. METHODS

We first present the encoding model used for spikes and LFP and the corresponding recursive multiscale decoder, which we have derived in our previous work [6]. We then describe the NHP experimental procedures [9] and the processing in extracting spikes and LFPs from the raw neural signals. Finally, we show how we fit the parameters of the multiscale decoder from experimental data and evaluate the performance of the multiscale decoder as a function of the number of LFP channels added to spikes. As our measure of performance, we use the correlation coefficient between the decoded and true trajectories.

A. The prior and multiscale observation models

We model the dynamics of movement as a linear random-walk process given by

$$\mathbf{x}_t = \mathbf{A}\mathbf{x}_{t-1} + \mathbf{w}_{t-1} \tag{1}$$

where $\mathbf{x}_t$ is the kinematic state to be decoded, $\mathbf{A}$ is the dynamics matrix, and $\mathbf{w}_{t-1}$ is a zero-mean white Gaussian noise with covariance matrix $\mathbf{W}$. To make the multiscale decoder generalizable across various types of movements, the dynamic matrix $\mathbf{A}$ is designed simply to enforce continuity in the evolution of kinematics.

As our observations, we use the recorded LFP and spikes. Previous work (e.g., [2]) has shown that some bands of the LFP power spectral density (PSD) encode motor intention. Also, recent work [8] has shown that modeling the spikes directly as a time-sequence of zeros and ones—indicating the lack or presence of spikes, respectively—using a point process could improve BMI performance. Hence we take the time-series of LFP log-power in various frequency bands and the zero and one time-series of spikes as our observations. LFP log-power features and binary spikes have some fundamental differences. First, LFP features are continuous-valued and spike time-series are discrete-valued. So these signals should be modeled using different likelihood functions. Second, LFP and spikes have different time-scales. For example, since PSD is calculated from LFPs using a moving window of finite length, its time-scale is often much slower than the millisecond time-scale of spikes. The multiscale decoder [6] takes into account all these differences by using a joint statistical likelihood model consisting of a combination of nonlinear point process and linear Gaussian models as presented below.

We take the log-power in various frequency bands as the LFP features. We characterize the LFP features using a linear Gaussian model

$$\mathbf{y}_t = \mathbf{C}\mathbf{x}_t + \mathbf{v}_t \tag{2}$$

where $\mathbf{y}_t$ includes all LFP features from all channels, $\mathbf{C}$ is a parameter matrix, and $\mathbf{v}_t$ is a zero-mean white Gaussian noise with covariance matrix $\mathbf{V}_t$.

We denote the binary spike event of neuron c at time t by N_t^c. Assuming that there are C total neurons, $N_t^{1:C} = [N_t^1, ..., N_t^C]'$ includes all spikes events at time t. We model the spike time-series for neuron c as a point process [10]–[13]

$$p(N_t^{1:C}|\mathbf{x}_t) = \prod_{c=1}^{C} (\lambda_c(t|\mathbf{x}_t)\Delta)^{N_t^c} \exp(-\lambda_c(t|\mathbf{x}_t)\Delta) \tag{3}$$

where Δ is the time-bin taken small enough to contain at most one spike and $\lambda_c(t|\mathbf{x}_t) = \exp(\beta_c + \boldsymbol{\alpha}_c'\mathbf{x}_t)$ is the firing rate of neuron c at time t. We also assume that LFP features and spikes are conditionally independent given the subject's motor intention $\mathbf{x}_t$, i.e.,

$$p(\mathbf{y}_t, N_t^{1:C}|\mathbf{x}_t) = p(\mathbf{y}_t|\mathbf{x}_t)\; p(N_t^{1:C}|\mathbf{x}_t) \tag{4}$$

where $p(\mathbf{y}_t|\mathbf{x}_t)$ and $p(N_t^{1:C}|\mathbf{x}_t)$ are given in (2) and (3), respectively. Thus the complete joint observation model in the multiscale decoder is given in (4).

B. Multiscale decoder

The multiscale decoder is derived from (1), (2), and (3) and consists of two steps: prediction and update. The derivation can be found in [6]. Denoting the prediction mean and covariance matrix by $\mathbf{x}_{t|t-1}$ and $\mathbf{Q}_{t|t-1}$, respectively, the prediction step is given by

$$\mathbf{x}_{t|t-1} = \mathbf{A}\mathbf{x}_{t-1|t-1} \tag{5}$$

$$\mathbf{Q}_{t|t-1} = \mathbf{A}\mathbf{Q}_{t-1|t-1}\mathbf{A}^T + \mathbf{W} \tag{6}$$

Similarly, denoting the posterior mean and covariance matrix by $\mathbf{x}_{t|t}$ and $\mathbf{Q}_{t|t}$, respectively, the update step is given by

$$\mathbf{Q}_{t|t}^{-1} = \mathbf{Q}_{t|t-1}^{-1} + \mathbf{C}^T\mathbf{V}_t^{-1}\mathbf{C} + \left[\sum_{c=1}^{C} \boldsymbol{\alpha}_c\boldsymbol{\alpha}_c^T\lambda_c(t|\mathbf{x}_t)\Delta\right]_{\mathbf{x}_{t|t-1}} \tag{7}$$

$$\mathbf{x}_{t|t} = \mathbf{x}_{t|t-1} + \mathbf{Q}_{t|t} \times \left[\mathbf{C}^T\mathbf{V}_t^{-1}\big[\mathbf{y}_t - \mathbf{C}\mathbf{x}_t\big]\right]_{\mathbf{x}_{t|t-1}} + \mathbf{Q}_{t|t} \times \left[\sum_{c=1}^{C} \boldsymbol{\alpha}_c\big[N_t^c - \lambda_c(t|\mathbf{x}_t)\Delta\big]\right]_{\mathbf{x}_{t|t-1}} \tag{8}$$

To address the different time-scales, i.e., that there are more samples of spikes compared with LFP features, we set the time-step of the multiscale decoder to that of the spikes. We then model the LFP features in time-steps in which they are not observed as missing. Mathematically, this is equivalent to setting the covariance matrix $\mathbf{V}_t \to \infty$ in the multiscale decoder for these time-steps. With this choice, the multiscale decoder specializes to a PPF [10] at the time-steps in which LFP features are not observed. Hence we can still run the decoder at the fast time-scale of the spikes (i.e., millisecond) and add information from the LFP observations when available. The decoder thus updates the estimate of kinematics at two time-scales, one corresponding to the spikes and the other corresponding to LFP.

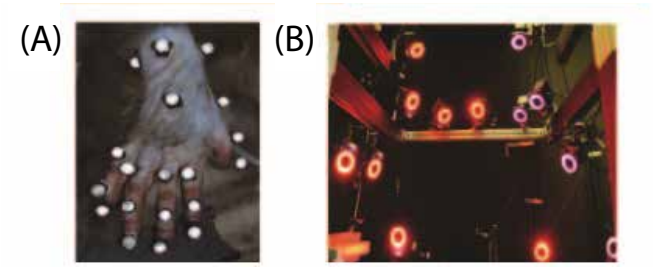

Fig. 1. Behavioral task setup. (A) Reflective markers on subject's skin. (B) Infrared and near-infrared cameras surrounding the workspace.

C. Experimental procedures and behavioral task

The subject is implanted with an electrode array (137 electrodes) over dorsal premotor cortex (PMd), ventral premotor cortex (PMv), and primary motor cortex (M1). The subject is trained to perform a reach and grasp task with their contralateral arm. 23 reflective markers were attached to the subjects skin and then tracked by multiple cameras as shown in Figure 1. The sampling rate of marker tracking is 100 frames/sec. Using the marker trajectories and a NHP musculoskeletal model [14], we can solve for the 27 arm joint angles through inverse kinematics. Our goal is to show that the multiscale decoder can improve the decoding of the joint angle trajectories compared with a PPF that only uses the spiking activity.

D. Data processing

The raw neural signal is recorded with a sampling frequency of 30 kHz. The spikes are extracted by passing the raw signal through a band-pass filter from 0.3–6.6 kHz and finding threshold crossings 3.5 standard deviations below the mean filtered signal. We bin the spikes with 10 ms bins to create the binary time-series. LFPs are obtained by low-pass filtering the raw signal with a 400 Hz cut-off frequency and then down-sampling the signal to 1 kHz. The PSD is calculated from LFPs with a causal 300 ms moving window every 50ms. So the sampling rate of PSD and spikes are 20 Hz and 100 Hz, respectively.

E. Decoding and performance evaluation

To show that the multiscale decoder can successfully add information from LFP to spikes, we simulate a realistic scenario with a typical implant. While implants can initially acquire single-unit or multi-unit spiking activity from the majority of electrodes, over time their recording quality could degrade. This degradation results in a loss of spiking activity from some channels. In contrast to spikes, LFP is more robust to signal degradation over time. Thus we consider a scenario in which the implant can still record spikes from 10 channels. We select these channels at random. We then examine whether the multiscale decoder can improve decoding performance by adding LFP from the rest of the channels. In particular, we examine the improvement in decoding as a function of the number of LFP channels added, where the LFP channels are also selected at random.

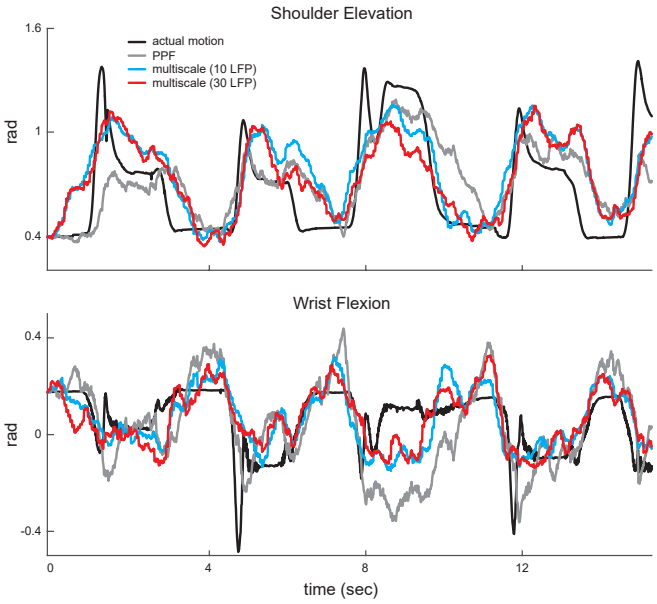

Fig. 2. Decoded trajectories of two joints using different decoders.

We decode the trajectory of each of the arm's 7 joints separately. These are shoulder elevation, elevation angle, shoulder rotation, elbow flexion, pro supination, wrist flexion, and wrist deviation. For each joint, the kinematic state $\mathbf{x}_t$ is taken as the joint angle at time t in radians. We enforce continuity by selecting $\mathbf{A} = 1$ and fitting $\mathbf{W}$ to the true trajectory using linear regression. The observation model, (2) and (3), is fitted using maximum-likelihood. For every combination of the 10 neurons and the randomly selected LFPs, we run a 20-fold cross-validation experiment over the whole dataset (300 sec). We take the correlation-coefficient between the decoded and the true joint trajectory as our measure of performance. Some examples of the decoded trajectories are shown in Figure 2.

We add the LFP channels in the multiscale decoder one by one, and evaluate how the correlation coefficient changes. Since LFP channels are selected randomly, we repeat the cross-validation process 50 times to find the average performance improvement. We also assess the improvement for each joint separately. The result is shown in Figure 3.

III. Results

Our goal is to show that the multiscale decoder could improve the performance of the PPF decoder by adding information from LFPs. We thus compare the decoding performance of the PPF and the multiscale decoder with various number of LFPs.

Figure 2 demonstrates example decoded trajectories from PPF and from the multiscale decoder. We can see that the multiscale decoder improves the tracking of joint angles by adding information from LFPs. Also, the similarity between tracking using 10 (cyan) and 30 LFP channels (red) indicates that a few LFP channels may be sufficient for this improved performance.

Figure 3 shows the average improvement of the multiscale decoder across 7 joints compared with the PPF decoder

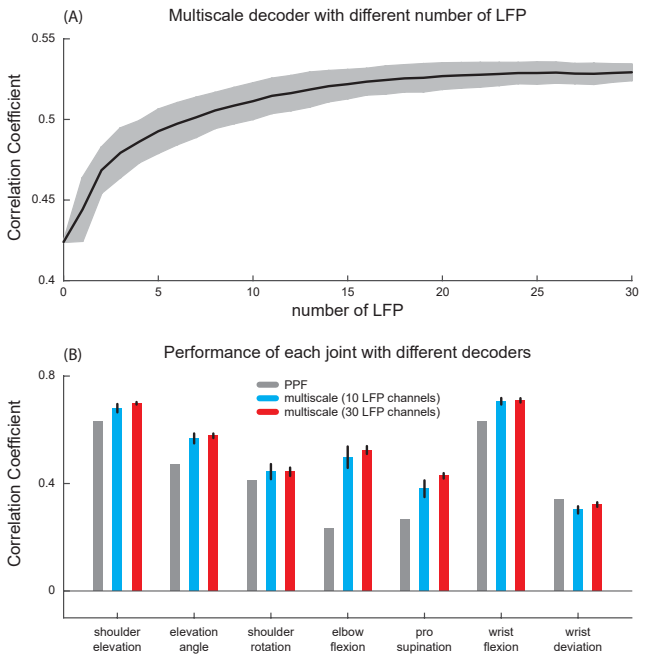

Fig. 3. Improvement of the multiscale decoder with different LFP (A) Improvement of multiscale decoder performance compared to PPF (which uses only spikes) as a function of the number of LFP channels added. Solid line shows the average improvement and shadows show the standard deviation. (B) Multiscale decoding improvement for each of the 7 joint angles. Bars show average performance and error bars indicate the standard deviation.

(which only uses spikes) as a function of the number of LFP channels added. The average and the standard deviation are obtained from the 50 experiments in which we add LFP channels one by one and at random. The correlation coefficient increases up to 10 LFP channels and then approximately saturates (Figure 3A). On average the improvement is 24.8% when adding 30 random LFP channels in the multiscale decoder and 21.3% when adding 10 random LFP channels to this decoder. We also examine the improvement in decoding performance for each joint separately (Figure 3B). We see that for all joint motions, except for the wrist deviation, the multiscale decoder works better than PPF (p-value $< 10^{-19}$).

IV. Conclusions

Improving BMI longevity is critical for clinical viability. Exploiting signal modalities such as LFP, which are more robust to signal degradation compared to spikes, could help enable reliable BMI performance over time. To simultaneously use LFP and spikes in BMIs, we need to develop multiscale decoders that account for the statistical and time-scale differences of these signals. We have developed such a multiscale decoder. Here, using NHP motor cortical LFP/spike recordings during a reach-to-grasp movement, we show that the multiscale decoder can add information from LFP to spikes while running at the fast time-scale of the spiking activity. In particular, the multiscale decoder improves the decoding accuracy of the NHP joint angles in the upper-arm. Correlation coefficients between the decoded and true joint angles (3D movement of 7 major joints) were improved by approximately 25% in the multiscale decoder compared to a single-scale PPF decoder, which only used the spiking activity. Moreover, the performance of the multiscale decoder approximately saturated using only 10 random LFP channels, showing the robustness of this approach. These results suggest that the multiscale decoder has the potential to improve the reliability of BMIs over time.

Acknowledgment

Support for this work was provided by ARO MURI Contract W911NF-16-1-0368, NSF CAREER Award CCF-1453868, and Cal-BRAIN Award 62636622.

References

[1] J. d. R. Milan and J. M. Carmena, "Invasive or noninvasive: Understanding brain-machine interface technology [conversations in bme]," *IEEE Engineering in Medicine and Biology Magazine*, vol. 29, no. 1, pp. 16–22, 2010.

[2] K. So, S. Dangi, A. L. Orsborn, M. C. Gastpar, and J. M. Carmena, "Subject-specific modulation of local field potential spectral power during brain-machine interface control in primates," *J. Neural Eng.*, vol. 11, p. 026002, Feb. 2014.

[3] D. A. Markowitz, Y. T. Wong, C. M. Gray, and B. Pesaran, "Optimizing the decoding of movement goals from local field potentials in macaque cortex," *J. Neurosci.*, vol. 31, pp. 18 412–18 422, Feb. 2011.

[4] R. D. Flint, C. Ethier, E. R. Oby, L. E. Miller, and M. W. Slutzky, "Local field potentials allow accurate decoding of muscle activity," *J. Neurophysiol.*, vol. 108, pp. 18–24, Feb. 2012.

[5] E. J. Hwang and R. A. Andersen, "Brain control of movement execution onset using local field potentials in posterior parietal cortex," *J. Neurosci.*, vol. 29, pp. 14 363–14 370, 2009.

[6] H.-L. Hsieh and M. M. Shanechi, "Multiscale brain-machine interface decoders," in *Engineering in Medicine and Biology Society (EMBC), 2016 IEEE 38th Annual International Conference of the*. IEEE, 2016, pp. 6361–6364.

[7] S. Stavisky, J. Kao, P. Nuyujukian, S. Ryu, and K. Shenoy, "Hybrid decoding of both spikes and low-frequency local field potentials for brain-machine interfaces," in *Engineering in Medicine and Biology Society (EMBC), 2014 36th Annual International Conference of the IEEE*, Aug 2014, pp. 3041–3044.

[8] M. M. Shanechi, A. L. Orsborn, H. G. Moorman, S. Gowda, S. Dangi, and J. M. Carmena, "Rapid control and feedback rates enhance neuroprosthetic control," *Nature Communications*, vol. 8, p. 13825, 2017.

[9] Y. T. Wong, D. Putrino, A. Weiss, and B. Pesaran, "Utilizing movement synergies to improve decoding performance for a brain machine interface," in *Engineering in Medicine and Biology Society (EMBC), 2013 35th Annual International Conference of the IEEE*. IEEE, 2013, pp. 289–292.

[10] M. M. Shanechi, A. L. Orsborn, and J. M. Carmena, "Robust brain-machine interface design using optimal feedback control modeling and adaptive point process filtering," *PLoS Comput Biol*, vol. 12, no. 4, p. e1004730, 2016.

[11] W. Truccolo, U. T. Eden, M. R. Fellows, J. P. Donoghue, and E. N. Brown, "A point process framework for relating neural spiking activity to spiking history, neural ensemble, and extrinsic covariate effects," *J. Neurophysiol.*, vol. 93, pp. 1074–1089, 2005.

[12] M. M. Shanechi, Z. M. Williams, G. W. Wornell, R. Hu, M. Powers, and E. N. Brown, "A real-time brain-machine interface combining motor target and trajectory intent using an optimal feedback control design," *PLOS ONE*, vol. 8, no. 4, p. e59049, Apr. 2013.

[13] H.-L. Hsieh and M. Shanechi, "Optimal calibration of the learning rate in closed-loop adaptive brain-machine interfaces," in *Proc. IEEE Conference on Engineering in Medicine and Biology Society (EMBC)*, Milan, Italy, Aug 2015, pp. 1667–1670.

[14] S. L. Delp, F. C. Anderson, A. S. Arnold, P. Loan, A. Habib, C. T. John, E. Guendelman, and D. G. Thelen, "Opensim: open-source software to create and analyze dynamic simulations of movement," *IEEE transactions on biomedical engineering*, vol. 54, no. 11, pp. 1940–1950, 2007.